Accepted Manuscript

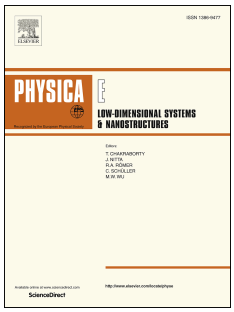

Nonlinear optical absorption and cyclotron–impurity resonance in monolayer silicene

N.V.Q. Binh, Nguyen N. Hieu, Chuong V. Nguyen, Huynh V. Phuc, Bui D. Hoi, Le T.T. Phuong, Tran C. Phong

PII: S1386-9477(18)30866-X

DOI: 10.1016/j.physe.2018.09.014

Reference: PHYSE 13288

To appear in: *Physica E: Low-dimensional Systems and Nanostructures*

Received Date: 9 June 2018

Revised Date: 31 August 2018

Accepted Date: 14 September 2018

Please cite this article as: N.V.Q. Binh, N.N. Hieu, C.V. Nguyen, H.V. Phuc, B.D. Hoi, L.T.T. Phuong, T.C. Phong, Nonlinear optical absorption and cyclotron–impurity resonance in monolayer silicene, *Physica E: Low-dimensional Systems and Nanostructures* (2018), doi: https://doi.org/10.1016/j.physe.2018.09.014.

This is a PDF file of an unedited manuscript that has been accepted for publication. As a service to our customers we are providing this early version of the manuscript. The manuscript will undergo copyediting, typesetting, and review of the resulting proof before it is published in its final form. Please note that during the production process errors may be discovered which could affect the content, and all legal disclaimers that apply to the journal pertain.

ACCEPTED MANUSCRIPT

Nonlinear optical absorption and cyclotron–impurity resonance in monolayer silicene

N.V.Q. Binh[a], Nguyen N. Hieu[a], Chuong V. Nguyen[b], Huynh V. Phuc[c], Bui D. Hoi[d,*], Le T.T. Phuong[e,*], Tran C. Phong[f]

[a] *Institute of Research and Development, Duy Tan University, 03 Quang Trung, Da Nang, Vietnam*
[b] *Department of Materials Science and Engineering, Le Quy Don Technical University, Ha Noi, Vietnam*
[c] *Division of Theoretical Physics, Dong Thap University, Dong Thap, Vietnam*
[d] *Department of Physics, University of Education, Hue University, Hue, Vietnam*
[e] *Center for Theoretical and Computational Physics, University of Education, Hue University, Hue, Vietnam*
[f] *The Vietnam National Institute of Educational Sciences, Hanoi, Vietnam*

Abstract

The magneto-optical transport properties in monolayer silicene subjected simultaneously to a perpendicular magnetic field and an electromagnetic wave (optical field) are theoretically studied. The nonlinear absorption coefficient is calculated using perturbation theory taking account of the electron–impurity scattering. The cyclotron–impurity resonance (CIR) is observed through the absorption spectrum. The photon energy at resonances is found to be proportional to the square root of magnetic field. This behaviour is similar to that in graphene but different from that in conventional low-dimensional semiconductors. The full width at half maximum (FWHM) of CIR peaks increases with increasing magnetic field by the laws FWHM [meV] $\approx 0.432\sqrt{B[\mathrm{T}]}$ and FWHM [meV] $\approx 0.215\sqrt{B[\mathrm{T}]}$ for one- and two-photon absorption, respectively. The obtained FWHM is about one order of magnitude smaller than it is in graphene monolayers. Moreover, the temperature dependence of the FWHM is similar to that in graphene but different from that in conventional low-dimensional semiconductors.

*Corresponding author. Tel: +84-979515588
Email addresses: buidinhhoi@hueuni.edu.vn (Bui D. Hoi), thuphuonghueuni@gmail.com (Le T.T. Phuong)

ACCEPTED MANUSCRIPT

Keywords: silicene, optical absorption, cyclotron resonance, electron–impurity interaction

1. Introduction

Silicene is a two-dimensional lattice of silicon atoms arranged in a plane of honeycomb structure similar to graphene, as shown in Fig. 1. The term *silicene* was introduced for the first time by Guzmán-Verri and Lew Yan Voon in a theoretical work studying electronic band structures of Si graphene-like sheets and Si nanotubes [1]. It was successfully fabricated on various substrates [2, 3, 4, 5, 6], just a few years after the Nobel Prize was awarded for the discovery of graphene. Because of its graphene-like structure, silicene possesses some special properties similar to those of graphene: charge carriers in silicene are the massless fermions described by the relativistic Dirac-like Hamiltonian, a linear energy dispersion near the Dirac points, high electron mobility (though smaller than graphene but much larger than silicon), and some others. Unlike graphene, silicene has a low-buckled structure resulted from the weak π bonding of the electrons in the outer shell [7]. Its band gap can be controlled by external perturbations, for example, electric field or magnetic fields. Also, the planar geometry in silicene is broken, leading to the strong spin-orbit interaction and forming a small energy gap (about 1.55 meV [55]). Although having similar physical properties, but for the potential applications in the near future, silicene is more advantageous than graphene because devices and technologies used today are being based on silicon technology, hence, silicene is more compatible with modern devices and technologies than graphene is. Therefore, silicene has attracted numerous attention recently.

It is well-known that the study of magneto-optical transport properties of materials is of great significance for applications in optoelectronic devices, especially for novel layered materials discovered recently that have many exotic physical properties. Among the well-known quantum effects, cyclotron resonance (CR) is an important spectral tool for determining the parameters of materials with high accuracy. From the analysis of resonance spectrum, one can obtain the effective mass of carriers, the distance between the Landau energy levels, the Lande factor (g-factor) and so on. When a CR process accompanies the phonon absorption/emission we have the so-called the phonon-assisted cyclotron resonance or cyclotron-phonon resonance (CPR)

ACCEPTED MANUSCRIPT

[9, 10, 11, 12, 13, 14, 15, 16]. This type of resonance is usually studied at high temperatures when electron–phonon interaction overwhelms other interactions (electron–electron, electron–impurity). In contrast, at low temperatures when the electron–impurity interaction is dominant, one can observe the cyclotron-impurity resonance (CIR) in which the electron–impurity interaction directly affects the probability of resonant absorption/emission of photons by electrons. The CPR and CIR have been studied intensively both theoretically and experimentally in bulk semiconductors and conventional low-dimensional structures [17, 18, 19, 20, 21, 22, 23, 24, 25, 26, 27, 28, 29, 30]. In particular, very recently the CPR has been investigated in novel atomically 2D materials such as graphene [15, 16, 31, 32] and monolayer molybdenum disulfide [33]. The CIR also has been studied in bulk and conventional low-dimensional semiconductors [19, 20, 34, 35, 36] and graphene [37, 38]. However, it has not attracted adequate attention in silicene as well as other 2D atomically thin materials up to date, especially on the theoretical aspect. Up to date, there have been some works dealing with the optical absorption in silicene-based structures [39, 40, 41]. However, in those works, the authors only considered the effects of the illustrated light, electric fields, exchange fields [39], and the substrate [40] on the optical absorption. The effect of an external static magnetic field was not included and, hence, the CR was not observed.

In this work, we theoretically investigate the magneto-optical absorption in monolayer silicene subjected simultaneously to a perpendicular static magnetic field and an electromagnetic wave (EMW). Our purpose is to make a comparison of the magneto-optical absorption properties in silicene and in other 2D structures (conventional semiconductor quantum wells, quantum wires, graphene, etc.) and set a theoretical basis for further experimental studies. Besides, it has been shown that the multi-photon absorption plays an important role in nonlinear optics and should be considered to have better estimations [42, 43, 44, 45, 46, 47, 48]. Therefore, we include both one- and two-photon absorption processes in this investigation. The effect of electron–impurity interaction is also taken into account at low temperature. The paper is organised as follows. In Sec. 2, we present briefly the electronic structure of monolayer silicene in a magnetic field. Sec. 3 gives briefly the derivation of the magneto-optical absorption coefficient (AC). Numerical results and discussion are presented in Sec. 4. Finally, concluding remarks are shown in Sec. 5.

2. Monolayer silicene in a perpendicular magnetic field

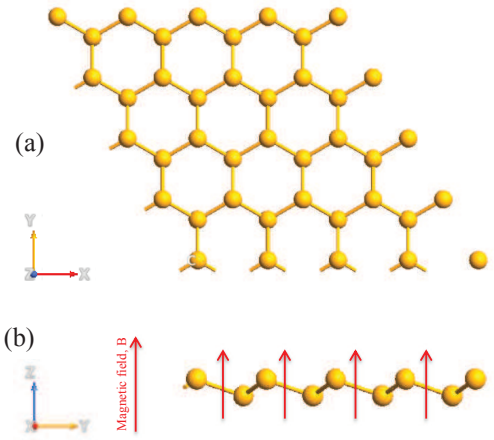

Figure 1: The top view (a) and side view (b) of the silicene sheet. Figure 1(b) shows the silicene sheet subjected to a perpendicular magnetic field which is considered in the present calculation.

In this calculation, we consider a silicence monolayer in which silicon atoms form a low-buckled honeycombs lattice as shown in Fig. 1. The silicene sheet is assumed to be placed in the $x-y$ plane. It was shown that the intrinsic spin-orbit interaction (SOI) is about ten times larger in magnitude than the Rashba SOI [49], so we can omit the Rashba term in the following calculations. In order to investigate the magneto-optical transport properties in silicene, we first recall its electronic band structure in a very general case when the material is subjected to a magnetic field (B) and a perpendicular electric field (E_z). The Hamiltonian matrix, $H_{\pm}$, for Dirac fermions in silicene reads [50, 51]

$$H_{\pm} = \begin{bmatrix} \lambda_{\pm}(s_z) & v_{\rm F}\pi_{\pm} \\ v_{\rm F}\pi_{\mp} & -\lambda_{\pm}(s_z) \end{bmatrix}, \tag{1}$$

where the $+$ $(-)$ sign corresponds to the K (K') valley, $v_{\rm F}$ is the Fermi velocity; $\pi_{\pm} = \pi_x \pm i\pi_y$, $\pi_{x(y)}$ is the x (y) component of the generalised momentum operator $\vec{\pi} = \vec{p} + e\vec{A}$, $\vec{p}$ is the momentum operator, $\vec{A}$ is the vector potential, and e is the electron charge; $\lambda_{\pm}(s_z) = \mp\lambda_{\rm SO}s_z + \ell E_z$, 2ℓ is the vertical distance between the two sub-lattices, $\lambda_{\rm SO}$ is the magnitude of

ACCEPTED MANUSCRIPT

the intrinsic SOI and $s_z = 1$ ($s_z = -1$) describes the up (down) spin. The Hamiltonian (1) is the relativistic Dirac-like Hamiltonian, similar to that in graphene [52].

When the magnetic field is oriented in the z direction ($\vec{B} = B\hat{e}_z$) with the Landau gauge $\vec{A} = (-By, 0, 0)$, the dimensionless Hamiltonian and its corresponding eigenvalues have been given in details in Ref. [51]. The energy spectrum for fermions in this case is

$$E^{\pm}_{n,s_z,p} = p\hbar\omega_c\Big\{n + \Big[\bar{\lambda}_{\pm}(s_z)\Big]^2\Big\}^{1/2}, \tag{2}$$

where $p = +1$ and $p = -1$, respectively, correspond to electrons and holes, $\omega_c = \sqrt{2}v_{\rm F}/\ell_B$, $\ell_B = \sqrt{\hbar/eB}$, $\bar{\lambda}_{\pm}(s_z) = \lambda_{\pm}(s_z)/\hbar\omega_c$, and $n(n >= 1)$ is the Landau level (LL) index. The associated spatial eigenfunctions of a fermion near the K valley are [51]

$$\psi^{+}_{n}(x) = \begin{pmatrix} \eta^{+}_{1}\phi_n(x) \\ \eta^{+}_{2}\phi_{n-1}(x) \end{pmatrix}, \tag{3}$$

with $\phi_n(x)$ being the normalised wave function of the harmonic oscillator and

$$\eta^{+}_{1} = \Big[\frac{\lambda_{+}(s_z) + E^{+}_{n,s_z,p}}{2E^{+}_{n,s_z,p}}\Big]^{1/2}, \tag{4}$$

$$\eta^{+}_{2} = -p\Big[\frac{-\lambda_{+}(s_z) + E^{+}_{n,s_z,p}}{2E^{+}_{n,s_z,p}}\Big]^{1/2}. \tag{5}$$

Similarly, one can write out the eigenfunctions near the K' valley as [51]

$$\psi^{-}_{n}(x) = \begin{pmatrix} \eta^{-}_{1}\phi_{n-1}(x) \\ \eta^{-}_{2}\phi_{n}(x) \end{pmatrix}, \tag{6}$$

with

$$\eta^{-}_{1} = -p\Big[\frac{\lambda_{-}(s_z) + E^{-}_{n,s_z,p}}{2E^{-}_{n,s_z,p}}\Big]^{1/2}, \tag{7}$$

$$\eta^{-}_{2} = \Big[\frac{-\lambda_{+}(s_z) + E^{-}_{n,s_z,p}}{2E^{-}_{n,s_z,p}}\Big]^{1/2}. \tag{8}$$

If we neglect the SOI term ($\lambda_{\rm SO}$) and take the vertical distance (2ℓ) to be zero, the Hamiltonian (1) is identical to that in graphene [52] and the energy

ACCEPTED MANUSCRIPT

spectrum (2) as well as wave functions (6) become that of graphene in a perpendicular magnetic field [52]. The similarity in the electronic properties of silicene and graphene comes from the fact that their lattice structures and electron configurations are similar. Both silicene and graphene are 2D materials with hexagonal lattices, also carbon and silicon elements belong to the group-IV elements. Mathematically, the electronic structure of both graphene and silicene around the Dirac point can be described by the similar relativistic Dirac-like Hamiltonians.

In the present calculation, we do not focus on the effect of the external electric field on the magneto-optical properties in silicene, so in the following we will consider the case of the absence of the electric field, i.e., $E_z = 0$ is taken in the above formulae. In the next section (Sec. 3), we present the derivation of the AC when an EMW propagates in the above-mentioned silicene monolayer.

3. Expression of the absorption coefficient

Let us consider the interaction of electrons in silicene with photons and ionized impurities that induces electron transitions between Landau magnetic subbands. The absorption coefficient, Γ^{ℓ}, for the ℓ-photon process can be written as [53]

$$\Gamma = \frac{16\pi\hbar n_0}{c\sqrt{\epsilon_\infty}\alpha_0^2\omega}\Big[1-\exp\Big(-\frac{\hbar\omega}{k_BT}\Big)\Big]\sum_{\alpha,\alpha'} f(E_\alpha)[1-f(E_{\alpha'})]W_{\alpha,\alpha'}, \qquad (9)$$

where we have denoted $E^{\pm}_{n,s_z,p} \equiv E_\alpha$ for simplicity, $f(E_\alpha)$ is the equilibrium Fermi-Dirac distribution for electrons, c is the speed of light in free space, ϵ_∞ is the high-frequency dielectric constant in silicene, n_0 is the electron density, $\alpha_0 = E_0/\omega$ with E_0 and ω, respectively, being the amplitude and frequency of the EMW (optical field). The sum in Eq. (9) is taken over all possible electron initial ($|\alpha\rangle$) and final ($|\alpha'\rangle$) states, and $W_{\alpha,\alpha'}$ is the transition probability due to carrier–photon–impurity interaction in silicene which has the form

$$W_{\alpha,\alpha'} = \frac{2\pi n_i}{\hbar S_0}\sum_{\ell,q}|U(q)|^2|J^{\pm}_{n,n',p,p'}(s_z)|^2\ell J^2_\ell(a_0q)\delta_{k_x,k'_x+q_x}\delta_{s_z,s'_z}\delta(E_\alpha - E_{\alpha'} - \ell\hbar\omega). \qquad (10)$$

Here, n_i is the concentration of impurities, S_0 is the area of the sample, q is the change in electron wave vector, $J_\ell(x)$ is the ℓ^{th}-order Bessel function of

ACCEPTED MANUSCRIPT

the argument x, $a_0 = eE_0/(2m^*(\omega^2-\omega_c^2))$ with m^* being the electron effective mass, $U(q)$ is the Fourier transform of the impurity potential. For the short-range scattering mechanism, which is considered in this investigation, the screened impurity potential is $U(q) = 2\pi U_0/q_s$ [51], where $U_0 = e^2/4\pi\epsilon_r\epsilon_0$, ϵ_r is the dielectric constant, ϵ_0 is the vacuum permittivity, q_s is the screening wave number which characterises the potential range of the scatterers. The form factor $|J^{\pm}_{n,n',p,p'}(s_z)|$ is given as follows [51]

$$|J^{+}_{n,n',p,p'}(s_z)|^2 = \frac{n_<!}{n_>!}u^{n_>-n_<}e^{-u}\Big[\eta_1^{+}\eta_1^{+'}L_{n_<}^{n_>-n_<}(u) + \eta_2^{+}\eta_2^{+'}\sqrt{\frac{n_<}{n_<}}L_{n_<-1}^{n_>-n_<}(u)\Big]^2, \tag{11}$$

$$|J^{-}_{n,n',p,p'}(s_z)|^2 = \frac{n_<!}{n_>!}u^{n_>-n_<}e^{-u}\Big[\eta_2^{-}\eta_2^{-'}L_{n_<}^{n_>-n_<}(u) + \eta_1^{-}\eta_1^{-'}\sqrt{\frac{n_>}{n_<}}L_{n_<-1}^{n_>-n_<}(u)\Big]^2, \tag{12}$$

with $u = \ell_B^2 q^2/2$, $n_< \equiv \min(n,n')$, $n_> \equiv \max(n,n')$, and $L_{n_<}^{n_>-n_<}$ being the associated Laguerre polynomial.

In this calculation, we consider both the one- and two-photon absorption ($\ell = 1, 2$). Also, in the Bessel functions appearing in Eq. (10) we limit ourself to the terms which depend on E_0 up to the second order, i.e., E_0^2. It should be noted that electron–impurity scattering can make electrons change their initial orbits and contribute to both the transition probability and absorption coefficient. Therefore, we evaluate this contribution by converting the summations over q, α, α' into the integrals

$$\sum_q \;\rightarrow\; \frac{S_0}{(2\pi\ell_B)^2}\int_0^{\infty} du \int_0^{2\pi} d\varphi, \tag{13}$$

$$\sum_{\alpha/\alpha'} \;\rightarrow\; \sum_{n,p,s_z,\pm/n',p',s_z',\pm} \frac{L_x}{2\pi}\int_{-L_y/2\ell_B^2}^{L_y/2\ell_B^2} = \frac{S_0}{2\pi\ell_B^2}\sum_{n,p,s_z,\pm/n',p',s_z',\pm}. \tag{14}$$

The integral over u can be calculated analytically using the orthogonality of the Laguerre polynomials. After a straightforward calculation, we obtain the AC for the K valley as

$$\begin{aligned}\Gamma^{+} \;=\; & \frac{32\pi^2 n_i n_0}{c\sqrt{\epsilon(\omega)}\alpha_0^2\omega\ell_B^2}\Big[1-\exp\Big(-\frac{\hbar\omega}{k_BT}\Big)\Big]\sum_{n,n'}\sum_{p,p'}\sum_{s_z,+} f(E^{+}_{n,s_z,p})[1-f(E^{+}_{n',s_z,p'})] \\ \times\; & \Big[I_1^{+}\delta(E^{+}_{n,s_z,p}-E^{+}_{n',s_z,p'}-\hbar\omega) + I_2^{+}\delta(E^{+}_{n,s_z,p}-E^{+}_{n',s_z,p'}-2\hbar\omega),\end{aligned} \tag{15}$$

ACCEPTED MANUSCRIPT

where

$$I_1^+ = \frac{S_0 U_0^2 a_0^2}{q_s^2 \ell_B^4}\Big[(\eta_1^+\eta_1^{+'})^2(n_> + n_< + 1) - 2\sqrt{n_< n_>}\eta_1^+\eta_1^{+'}\eta_2^+\eta_2^{+'} + (\eta_2^+\eta_2^{+'})^2(n_> + n_< - 1)\Big], \quad (16)$$

$$I_2^+ = \frac{S_0 U_0^2 a_0^4}{q_s^2 \ell_B^6}\Big[(\eta_1^+\eta_1^{+'})^2\Big[2 + 6n_<(n_< + 1) + (n_> - n_<)(n_> + 5n_< + 3)\Big] - 4\sqrt{n_< n_>}\eta_1^+\eta_1^{+'}\eta_2^+\eta_2^{+'}(n_> + n_<) + (\eta_2^+\eta_2^{+'})^2\Big[2 + 6n_<(n_< - 1) + (n_> - n_<)(n_> + 5n_< - 3)\Big]\Big]. \quad (17)$$

Similarly, the results for the K' valley are given by Eqs. (15) - (17) with $E^+_{n,s_z,p}$ and η_1^+ replaced by $E^-_{n,s_z,p}$ and η_2^-, respectively.

4. Numerical analysis and discussion

Now we perform numerical calculations of the above results to clarify some physical behaviours of the absorption spectrum in monolayer silicene. The parameters used in the calculations are as follows [51, 54, 55]: $E_0 = 10^5$ V/m, $n_0 = 5 \times 10^{15}$ m^{-2}, $n_i = 10^{13}$ m^{-2}, $\epsilon_r = 4$, $v_{\rm F} = 5.42 \times 10^5$ m.s^{-1}, $\lambda_{\rm SO} = 3.9$ meV [51], and $q_s = 5 \times 10^8$ m^{-1} [51]. Because the K and K' valleys are equivalent so in the following we only consider the processes that take place within the K valley, i. e, the AC given by Eq. (15) is numerically calculated ($\Gamma^+ \equiv \Gamma$). Also, to eliminate the divergence of the delta functions in Eq. (15), we replace them by Lorentzians of the width parameter $\gamma = 0.01\hbar\omega_{\rm c}$ [51].

Figure 2 shows the absorption spectrum as a function of the photon energy at $B = 10$ T. In this figure, we can see clearly six maximum peaks labelled (1) to (6). These peaks are located, respectively, at the photon energy of $\hbar\omega_{(1)} = 9.8806$ meV, $\hbar\omega_{(2)} = 12.8691$ meV, $\hbar\omega_{(3)} = 19.7612$ meV, $\hbar\omega_{(4)} = 22.7498$ meV, $\hbar\omega_{(5)} = 25.7383$ meV, $\hbar\omega_{(6)} = 45.4995$ meV. These values of photon energy are shown to satisfy the following relations:

$$E_{3,1,1} - E_{2,1,1} = 2\hbar\omega_{(1)} \quad (18)$$

$$E_{2,1,1} - E_{1,1,1} = 2\hbar\omega_{(2)} \quad (19)$$

$$E_{3,1,1} - E_{2,1,1} = \hbar\omega_{(3)} \quad (20)$$

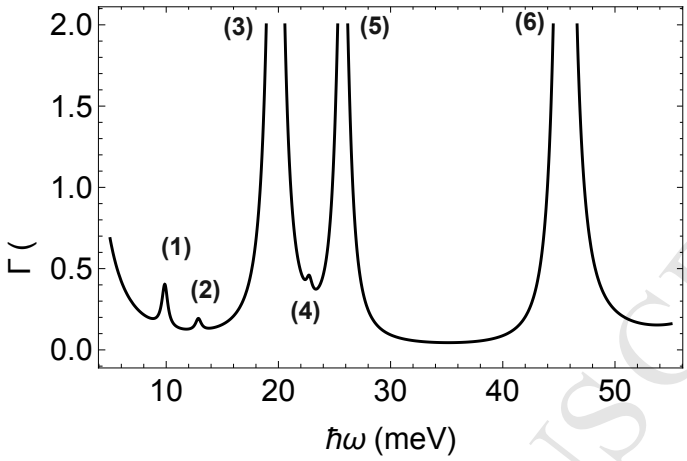

Figure 2: The AC as a function of the photon energy at $B = 10$ T and $T = 4.2$ K.

$$E_{3,1,1} - E_{1,1,1} = 2\hbar\omega_{(4)} \quad (21)$$

$$E_{2,1,1} - E_{1,1,1} = \hbar\omega_{(5)} \quad (22)$$

$$E_{3,1,1} - E_{1,1,1} = \hbar\omega_{(6)} \quad (23)$$

These relations are actually the CR conditions which have the general formula $\Delta E = \ell\hbar\omega$ where ΔE is the electron energy difference between the initial and final Landau states, $\ell = 1$ and $\ell = 2$ are, respectively, for one-photon (linear) and two-photon (nonlinear) absorption. The CR describes the electron transfer between the Landau energy levels through absorption/emission of photons. In Fig. 2, peaks (3), (5), and (6) correspond to one-photon processes and peaks (1), (2), and (4) correspond to two-photon processes. In this investigation, electron–impurity scattering also contributes to the electron transitions. Therefore, these peaks may be called CIR peaks. We also can see an important thing in Fig. 2 that the AC at two-photon CIR peaks is much smaller than that at one-photon CIR peaks. This implies the fact that the two-photon processes have a minor contribution to the absorption spectrum in comparison with the one-photon ones. However, it was shown that the multi-photon absorption has a significant role in nonlinear optics [42, 43, 44, 45, 46, 47, 48]. Experimentally, the two-photon absorption can be observed by using two-photon excited fluorescence (TPEF) introduced by Denk, Strickler, and Webb [48] where a Ti-sapphire laser is used to generate a photon beam with high density and flux required for two-photon absorp-

ACCEPTED MANUSCRIPT

tion, also its wavelength is tunable for a wide range. The TPEF has been considered as a standard technique in modern microscopy and used widely in many studies [56, 57, 58, 59, 60, 61]. Besides, it should be noted that we need a strong magnetic field to observe the CR. This requirement is easily met by using superconducting magnets used in observing, for example, the quantum Hall effect or other magneto-transport properties [62, 63].

To show the effect of the magnetic field on the absorption spectrum, in Fig. 3 we plot the AC versus photon energy absorption at $B = 10$ T (the solid curve) and $B = 5$ T (the dashed curve). It is seen that the magnetic field has a strong influence on the absorption spectrum. In fact, the value of the AC and the position of the CIR peaks vary strongly with the change of B. To be more specific, we consider the one-photon term in the AC. Fig. 4 shows the 3D plot of the AC versus the magnetic field and photon energy for the case of one-photon absorption. From the figure we can see that when the magnetic field increases, the value of the photon energy satisfying the cyclotron resonance condition, denoted $\hbar\omega_{\rm res}$, increases. The relation between $\hbar\omega_{\rm res}$ and B is numerically extracted and shown more clearly in Fig. 5. One can find that the resonant photon energy varies with the magnetic field by the law $\hbar\omega_{\rm res} \propto B^{1/2}$. So far, we can conclude that the dependence of the resonant photon energy on the magnetic field is similar to that in graphene [31, 37, 38] and is completely different from that in traditional low-dimensional semiconductors. This is originated from the fact that Landau energy in both graphene and silicene is proportional to $B^{1/2}$, whereas in traditional semiconductors it is proportional to B.

Beside the AC, the full width at half maximum (FWHM) of a resonant peak is also an important parameter in studying a resonant absorption. The FWHM is related to the electron transition probability in a resonant scattering process. The FWHM is defined to be the width of a resonant peak at the height equal to half of its maximum. To show the effect of the magnetic field on the FWHM of CIR peaks we now determine the FWHM as a function of the magnetic field. Figure 6 shows the contour plot of the AC versus the photon energy and magnetic field for the same transitions as in Figs. 4 and 5. Looking carefully at this figure, we find that the width of the all CIR peaks increases with increasing magnetic field. For more details, as an example, we compute the FWHM of the CIR peak corresponding to the transition $n = 1 \to n' = 2$ at different values of B. The B-dependent FWHM is shown in Fig. 7 for both one-photon absorption (filled squares) and two-photon absorption (filled circles). The figure shows that the FWHM

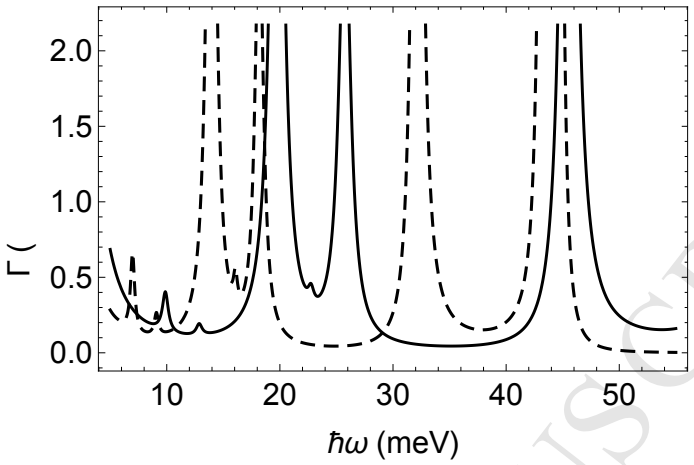

Figure 3: The same dependence as Fig. 1 for $B = 10$ T (solid curve) and $B = 5$ T (dashed curve).

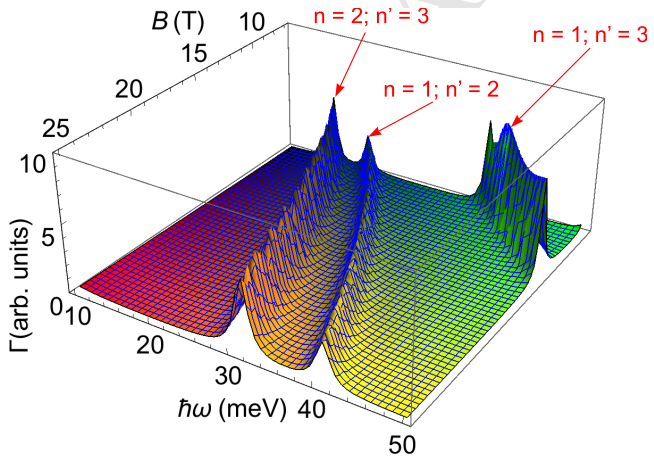

Figure 4: The 3D plot of the AC versus magnetic field and photon energy for some electron transitions. Here, only the one-photon absorption term in the AC is taken ($\ell = 1$) and $T = 4.2$ K.

increases with increasing B for both cases of absorption. The best fitting results show the laws for the B-dependent FWHMs for one- and two-photon absorption, respectively, as FWHM [meV] $\approx 0.432\sqrt{B[\mathrm{T}]}$ and FWHM [meV] $\approx 0.215\sqrt{B[\mathrm{T}]}$. It was also shown for graphene monolayers that the FWHM

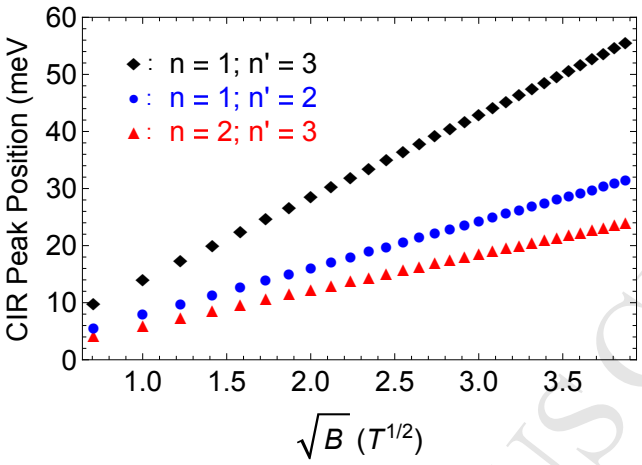

Figure 5: Relation between the photon energy at resonances and magnetic field in the case of one-photon absorption for some electron transitions. The other parameters are the same as in Fig. 4.

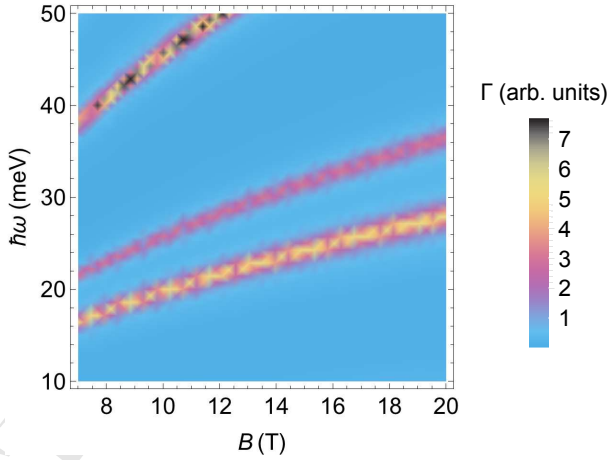

Figure 6: Density plot of the AP as a function of the photon energy and magnetic field for the same parameters as in Figs. 4 and 5.

is proportional to $\sqrt{B}$ [37, 38]. However, the FWHM in silicene is about one order of magnitude smaller than it is in graphene [37, 38] for the same ranges of magnetic field and temperature. The increase of the FWHM with magnetic field is reasonable and consistent with that explained in bulk and traditional

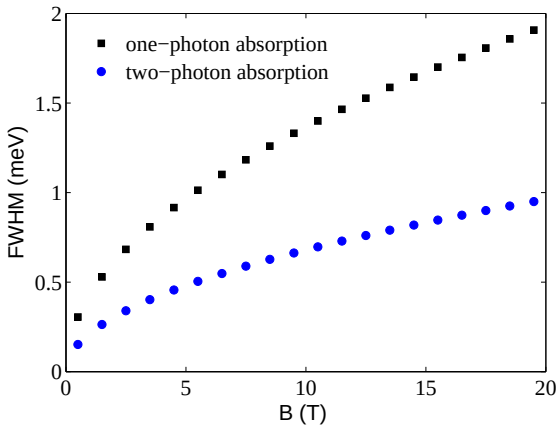

Figure 7: The FWHM as a function of magnetic field for $n = 1 \rightarrow n' = 2$ transition. Here, $T = 4.2$ K.

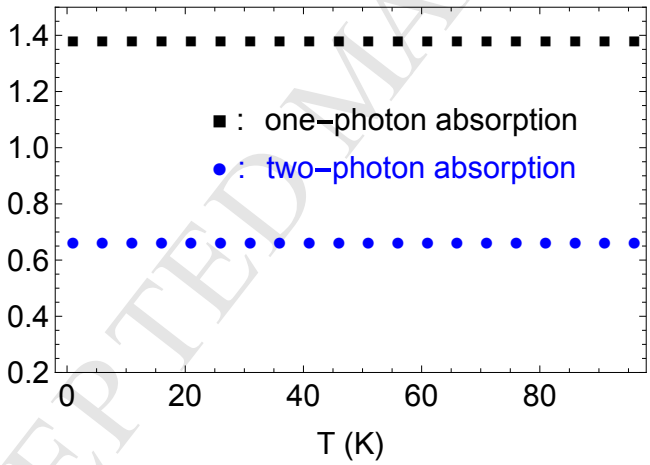

Figure 8: Dependence of the FWHM on the temperature at $B = 10$ T for $n = 1 \rightarrow n' = 2$ transition.

low-dimensional semiconductors [19, 20, 34, 35, 36] and in graphene [37, 38]. From Fig. 7, we can see one more interesting thing that the FWHM for the two-photon process is smaller than that for one-photon process. For example, at $B = 10$ T the FWHM for two-photon absorption is about 50% of that for one-photon absorption. This shows that the probability of two photons

ACCEPTED MANUSCRIPT

absorbing is smaller than the absorption of one photon.

The effect of temperature on the FWHM of CIR peaks is also considered. Fig. 8 shows the FWHM as a function of temperature. We can see from the figure that the FWHM apparently remains unchanged with increasing the temperature for the range from 0.1 K to 100 K. This behaviour implies that the scattering processes in silicene monolayer are very weakly thermally activated. The very weak dependence of the FWHM on temperature was also observed in graphene monolayers [31, 32], showing the similarity in the effect of temperature on the magneto-optical absorption properties of graphene and silicene monolayers.

5. Conclusions

We have calculated the nonlinear AC in silicene monolayer subjected to a perpendicular magnetic field, taking account of the electron–impurity scattering. The nonlinear AC has been considered as functions of the photon energy, the magnetic field, and the temperature. The CIR effect has been observed in the absorption spectra. The results show that the photon energy at CIR peaks is linearly proportional to the square root of magnetic field, which is similar to graphene and different from conventional semiconductors. For $n = 1 \to n' = 2$ transition, we find that the FWHM of CIR peaks increases with increasing magnetic field by the laws FWHM [meV] $\approx 0.432\sqrt{B[\mathrm{T}]}$ and FWHM [meV] $\approx 0.215\sqrt{B[\mathrm{T}]}$ for one- and two-photon absorption, respectively. In particular, the FWHM in silicene is independent on the temperature, showing the similarity to graphene monolayers and difference from conventional low-dimensional semiconductors.

Acknowledgement

This research is funded by Vietnam National Foundation for Science and Technology Development under grant number 103.01-2016.83.

References

[1] Gian G. Guzmán-Verri and L. C. Lew Yan Voon, Phys. Rev. B 76, 075131 (2007).

[2] P. Vogt et al., Phys. Rev. Lett. 108, 155501 (2012).

ACCEPTED MANUSCRIPT

[3] B. Augray, A. Kara, S. B. Vizzini, H. Oughaldou, C. LéAndri, B. Ealet, G. Le Lay, App. Phys. Lett. 96 (2010) 183102.

[4] A. Fleurence, R. Friedlein, T. Ozaki, H. Kawai, Y. Wang, and Y. Takamura, Phys. Rev. Lett. 108, 245501 (2012)

[5] L. Meng, Y. Wang, L. Zhang, S. Du, R. Wu, L. Li, Y. Zhang, G. Li, H. Zhou, W. A. Hofer, and M. J. Gao, Nano Lett. 13, 685 (2013).

[6] Meng Lei et al., Chinese Phys. B 24, 086803, (2015).

[7] Xiaodong Li, Jeffrey T. Mullen, Zhenghe Jin, Kostyantyn M. Borysenko, M. Buongiorno Nardelli, and Ki Wook Kim, Phys. Rev. B 87, 115418 (2013).

[8] Cheng-Cheng Liu, Wanxiang Feng, and Yugui Yao, Phys. Rev. Lett. 107, 076802 (2011).

[9] F. G. Bass and I. B. Levinson, Zh. Eksper. Teor. Fiz. 49, 914 (1965).

[10] B. D. McCombe, S. G. Bishop and R. Kaplan, Phys. Rev. Letters 18, 748 (1967).

[11] V. I. Ivanov-Omskii, L. I. Korovin, and E. M. Shereghii, Phys. Stat. Sol. (b) 90, 11 (1978).

[12] B. Tanatar and M. Singh, Phys. Rev. B 42, 3077 (1990).

[13] J. S. Bhat, B. G. Mulimani, and S. S. Kubakaddi, Phys. Rev. B 49 (1994) 16459.

[14] Huynh VinhPhuc, Nguyen Dinh Hien, Le Dinh, and Tran Cong Phong, Superlattices and Microstructures 94 (2016) 51.

[15] Huynh Vinh Phuc and Le Dinh, Materials Chemistry and Physics 163 (2015) 116.

[16] Huynh Vinh Phuc and Nguyen Ngoc Hieu, Opt. Commun. 344 (2015) 12.

[17] J. S. Bhat, S. S. Kubakaddi, and B. G. Mulimani, J. Appl. Phys. 70 (1991) 2216.

ACCEPTED MANUSCRIPT

[18] A. Suzuki and D. Dunn, Phys. Rev. B 25 (1982) 7754.

[19] D. Dunn and A. Suzuki, Phys. Rev. B 29 (1984) 942.

[20] C. K. Sarkar and R. J. Nicholas, J. Phys. C: Solid State Phys. 18 (1985) 1495.

[21] M. P. Chaubey and C. M. Van Vliet, Phys. Rev. B 34 (1986) 3932.

[22] R. J. Nicholas et al., Phys. Rev. B 45, 12144(R) (1992).

[23] N. L. Kang et al., J. Phys.: Condens. Matter 7 (1995) 8629.

[24] Y. J. Cho, N. L. Kang, K. S. Bae, J. Y. Ryu, and S. D. Choi, J. Phys.: Condens. Matter **8** (1996) 6957.

[25] W. Xu and C. Zhang, Phys. Rev. B 54 (1996) 4907.

[26] A. Suzuki and M. Ogawa, J. Phys.: Condens. Matter 10 (1998) 4659.

[27] S. C. Lee, H. S. Ahn, D. S. Kang, S. O. Lee, S. W. Kim, Phys. Rev. B 67, 115342 (2003).

[28] S. C. Lee, J. Korean. Phys. Soc. 51 (2007) 1979.

[29] X. G. Wu, F. M. Peeters, Y. J. Wang, and B. D. McCombe, Phys. Rev. Lett. 84 (2000) 4934.

[30] W. Y. Wang and W. Xu, Phys. Rev. B 86 (2012) 045307.

[31] M. Orlita et al., Phys. Rev. Lett. 101 (2008) 267601.

[32] Bui Dinh Hoi, Le Thi Thu Phuong, and Tran Cong Phong, J. Appl. Phys. 123 (2018) 094303.

[33] Chuong V. Nguyen, Nguyen N. Hieu, Nikolai A. Poklonski, Victor V. Ilyasov, Le Dinh, Tran C. Phong, Luong V. Tung, and Huynh V. Phuc, Phys. Rev. B 96 (2017) 125411.

[34] V. A. Margulis, J. Exp. Theor. Phys. 99 (2004) 633.

[35] J. Lee, E. S. Koteles, and M. O. Vassell, Phys. Rev. B 33 (1986) 5512.

ACCEPTED MANUSCRIPT

[36] T. Unuma, M. Yoshita, T. Noda, and H. Sakaki, J. Appl. Phys. 93 (2003) 1586.

[37] Z. Jiang, E.A. Henriksen, L.C. Tung, Y.-J. Wang, M.E. Schwartz, M.Y. Han, P. Kim, H.L. Stormer, Phys. Rev. Lett. 98 (2007) 197403.

[38] C. H. Yang, F. M. Peeters, and W. Xu, Phys. Rev. B 82 (2010) 205428.

[39] P. Chantngarm, K. Yamada, and B. Soodchomshom, J. Magn. Magn. Mater. 429 (2017) 16.

[40] E. Cinquanta et al., Phys. Rev. B 92 (2015) 165427.

[41] Xue-Sheng Ye, Zhi-Gang Shao, Hongbo Zhao, Lei Yang and Cang-Long Wang, RSC Adv. 4 (2014) 37998.

[42] J. A. Giordmaine, P. M. Rentzepis, S. L. Shapiro, and K. W. Wecht, Appl. Phys. Lett. 11 (1967) 216.

[43] F.G. Omenetto, W.A. Schroeder, K. Boyer, J.W. Longworth, A. McPherson, C.K. Rhodes, Appl. Opt. 36 (1997) 3421.

[44] M. Rasmusson, A.N. Tarnovsky, E. kesson, V. Sundstrm, Chem. Phys. Lett. 335 (2001) 201.

[45] J.I. Dadap, G.B. Focht, D.H. Reitze, M.C. Downer, Opt. Lett. 16 (1991) 499.

[46] G.S. He, P.P. Markowicz, T.C. Lin, P.N. Prasad, Nature 415 (2002) 767.

[47] A. Mukherjee, Appl. Phys. Lett. 62 (1993) 3423.

[48] W. Denk, J. H. Strickler, and W. W. Webb, Science 248 (1990) 73.

[49] M. Ezawa, Phys. Rev. Lett. 109 (2012) 055502.

[50] C. J. Tabert and E. J. Nicol, Phys. Rev. B 88 (2013) 085434.

[51] Kh. Shakouri, P. Vasilopoulos, V. Vargiamidis, and F. M. Peeters, Phys. Rev. B 90 (2014) 125444.

[52] A. H. Castro Neto, F. Guinea, N. M. R. Peres, K. S. Novoselov and A. K. Geim, Rev. Mod. Phys. 81 (2009) 109.

ACCEPTED MANUSCRIPT

[53] V. A. Margulis, Fiz. Tekh. Poluprovodn. (Leningrad) 17 (1983) 910 [Sov. Phys. Semicond. 17 (1983) 571].

[54] C.-C. Liu, H. Jiang, and Y. Yao, Phys. Rev. B 84 (2011) 195430.

[55] C.-C. Liu, W. Feng, and Y. Yao, Phys. Rev. Lett. 107 (2011) 076802.

[56] M. A. Albota, C. Xu, and W. W. Webb, Applied Optics 37(31) (1998) 7352.

[57] R. A. Negres et al., IEEE Journal of Quantum Electronics 38(9) (2002)1205.

[58] A. El Amili, G. Kervella, and M. Alouini, Optics Express 21(7) (2013) 8773.

[59] K. Matczyszyn et al., The Journal of Physical Chemistry B 119(4) (2015) 1515.

[60] A. Dragonmir, J. G. McInerney, and D. N. Nikogosyan,Applied Optics 41(21) (2002) 4365.

[61] J. Bewersdorf, P. Rainer, and S. W. Hell,Optics Letters 23 (1998) 665.

[62] M. N. Wilson, Superconducting Magnets (Monographs on Cryogenics), Oxford University Press (New edition), Oxford, 1987.

[63] M. O. Goerbig, Ultracold Gases and Quantum Information in *Lecture Notes of the Les Houches Summer School in Singapore*, Volume 91, Oxford, 2011.

ACCEPTED MANUSCRIPT

ACCEPTED MANUSCRIPT

Highlights

- The cyclotron-impurity resonance (CIR) is observed in the absorption spectra.
- The photon resonant energy is linearly proportional to the square root of magnetic field.
- The FWHM increases with increasing the magnetic field similarly to graphene.
- The FWHM is about one order of value smaller than it is in graphene.
- The FWHM is independent on temperature.

ACCEPTED MANUSCRIPT